SELF-CONSISTENT KLYSTRON SIMULATIONS*

B. E. Carlsten and P. J. Tallerico, AT-5, MS H827
Los Alamos National Laboratory, Los Alamos, NM 87545 USA

Summary

A numerical analysis of large-signal klystron behavior based on general wave-particle interaction theory is presented. The computer code presented is tailored for the minimum amount of complexity needed in klystron simulation. The code includes self-consistent electron motion, space-charge fields, and intermediate and output fields. It also includes use of time periodicity to simplify the problem, accurate representation of the space-charge fields, accurate representation of the cavity standing-wave fields, and a sophisticated particle-pushing routine. In the paper, examples are given that show the effects of cavity detunings, of varying the magnetic field profile, of electron beam asymmetries from the gun, and of variations in external load impedance.

Introduction

Klystrons are widely used as microwave power sources for accelerators and other devices requiring intense microwave fields. Usually, the dc power supplied to the klystrons is a major expense in the operation of these devices. As a result, higher, dc to rf-power-conversion efficiencies are sought for these klystrons. Analytic and numerical analysis is required to optimize klystron efficiency because experimental optimization is very expensive and time-consuming. The klystron is an electron-beam device in which the beam interacts with standing-wave rf fields in several consecutive and collinear rf cavities. Klystrons belong to the general group of beam/wave interaction devices.

The physics associated with modulation of the beam phase space by the cavities is a nonlinear beam/wave interaction. There is no satisfactory analytic solution describing this interaction for cavity modulation ratios greater than ~0.1 (the cavity voltage normalized to the beam voltage) and for modulation ratios that increase by a factor less than ~6 dB per cavity. The most satisfactory analyses of klystrons are done with numerical simulation models in which representative electrons in the beam are followed. However, most analyses are either too simplified to contain all the physics necessary for giving insight into the beam-dynamics process, particularly at high modulation levels, or they do not use inherent symmetries in the problem and as a consequence are too cumbersome.

A satisfactory, numerical-simulation computer code is based on a large-signal model that, when implemented, includes the following parts:

- Self-consistent electron motion
- Self-consistent space-charge fields
- Self-consistent intermediate and output cavity rf fields
- Accurate representation of the space-charge fields
- Accurate representation of the cavity-standing-wave rf fields
- Sophisticated particle-pushing algorithm
- Relaxation methods for convergence of self-consistent iterations
- Use of time periodicity to simplify the calculations

*Work supported by the Los Alamos National Laboratory Institutional Supporting Research and Development.

The first five points are needed to describe the necessary physics; the last three are useful in keeping the problem tractable. All points are tied together. The self-consistency of the first two points refers to maintaining the self-consistency of following only one dynamic rf wavelength of particles. The steady-state, large-signal computer-simulation code described in this paper includes all the above points. The code has an average computer running time of about 5 min CPU time on a CDC 7600 and has become a useful design tool.

Description of the Code

The model used is similar to the one we reported earlier[1] with added improvements and modifications to ensure self-consistency. A segment of beam one rf wavelength long is followed dynamically (as discussed in the next section) with time as the independent paramenter. This segment is divided into n_z equal axial divisions with each axial division divided into n_r equal-volume rings (where the innermost ring is a disk). The fully relativistic equations of motion are then solved for each of the rings as they are transported along the klystron, interacting with both cavity fields and mutual space-charge fields.

Calculation of the cavity rf fields is straightforward. The field distribution of the axially symmetric driven mode in the klystron's cavities can be found with the cavity mode program SUPERFISH.[2] The proper normalization for the field magnitude can be found from the cavity gap voltage using cylindrical coordinates

$$V_{gap}(t) = \int_{-\infty}^{\infty} \vec{E}_{cavity}(r = 0,z,t) \cdot d\hat{z} \quad , \tag{1}$$

where the cavity gap voltage also equals

$$V_{gap} = i_{ind_1} Z_{cav} \quad . \tag{2}$$

Here, Z_{cav} is the cavity impedance, given by

$$1/Z_{cav} = 1/R_{sh} + j(f/f_o - f_o/f)/(R_{sh}/Q), \tag{3}$$

where R_{sh} and R_{sh}/Q are measurable quantities, f is the frequency at which the mode is driven, and f_o is the mode's resonant frequency. Effects of external loading (especially for the output cavity) can be included using Eq. (2).The driving current is i_{ind_1} the fundamental Fourier component of the induced current given by Ramo's theorem:

$$i_{ind}(t)\ V_{gap}(t) = \int_V \vec{J}\ (t) \cdot \vec{E}_{cavity}(r,z,t)\ d_x^3 \quad ,$$

where the integral is over the cavity's volume. Equations (3)-(4) are correct to lowest order in 1/Q from a normal-mode field expansion.[3] The cavity fields must be self-consistent with the beam dynamics.

Space-charge fields are calculated as described before,[1] using propagator functions for the fields at an observer point (r,z) from a ring of uniform charge density at (r',z') with axial length dz and radial thickness dr. The exact space-charge-field expressions can be found in Ref. 2. In addition, space-charge fields must be self-consistent because the electrons in front of and behind the rf wavelength tracked contribute to the space-charge fields.

0018-9499/85/1000-2837$01.00© 1985 IEEE

With knowledge of both the cavity rf fields and the space-charge fields, particle motion is easy to calculate. An external magnetic field can be included in the calculations if necessary.

Self-Consistent Iteration Schemes

Particle motion through the klystron must be iterated to ensure satisfaction of three requirements of steady-state behavior. For the first requirement, an iteration must be made over each gap region to ensure that the induced current found in each gap (Eq. 4) is the same as the induced current drive (Eq. 2). If space-charge forces are significant, iterations are needed for the two other requirements. Certain particles, those corresponding to the initial one rf wavelength of the beam, are tracked; that is, their trajectories are calculated. All other particles are not initially tracked. If there is an axial-position reordering of particles so that particles not followed become close to and interact with those followed (Fig. 1), the space-charge fields calculated from the followed particles will be incomplete. This problem is taken care of automatically by following a dynamic rf wavelength of particles in which we follow new particles as they enter and quit following others as they leave the wavelength. The third requirement for using iterations comes from calculating the space-charge fields from particles in front of and behind the rf wavelength. It is necessary to store all particle positions for all time steps to get the correct so-called "edge" space-charge effects for subsequent iterations. Iteration schemes for the first and third requirements are obvious. However, the algorithm for dealing with the new dynamic rf wavelength will be explained further.

Before reordering:

particle number:	1	2	3	4	5	6	7	8	9	10	11	12

initial rf wavelength

After reordering:

particle number:	7	1	2	8	9	5	4	3	10	11	6	12

rf wavelength is ambiguous

Fig. 1. Reordering of particles occurs when some particles overtake others. When this happens, the initial rf wavelength (here shown as Particles 4 through 9) loses its continuity.

The new dynamic rf wavelength used in the simulation lets new particles be followed (if they enter) and lets current ones be forgotten (if they leave). This technique simplifies the space-charge-field calculations when particle overtaking occurs. This must be done self-consistently.

The leading edge to the wavelength is defined as the position of the particle tracked with the largest z-value. The trailing edge is at the same position as was the leading edge for the wavelength one rf period earlier. Then, as particles slow down, the trailing edge can catch up and pass them. From this point of view, the particles are lost into the dynamic wavelength behind the current one. This second wavelength must be identical to the one being tracked one period earlier in time. From the other point of view, as a dynamic wavelength catches up to a slower particle in the dynamic wavelength ahead of it, it absorbs the new particle (Fig 2). At any instant, there is a series of well-defined rf wavelengths that are stacked one after another and that represent the entire length of the beam. Although at that instant only one of these rf wavelengths is followed by the simulation,

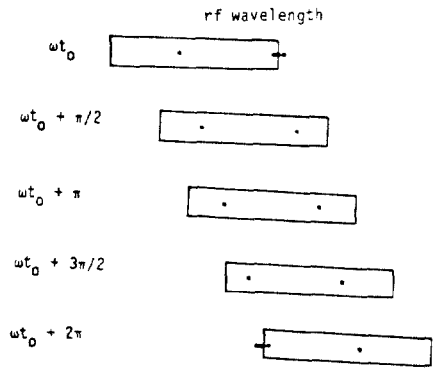

Fig. 2. Particles can enter and leave the rf wavelength. Any particle entering at time t_0 must correspond to another leaving exactly one period later.

it has been or will become identical to all the other wavelengths at a multiple of periods earlier or later, from the time periodicity. From Fig. 2, it is also clear that although a dynamic wavelength may contain two particles related by the fact that they started out exactly one period apart with otherwise identical boundary conditions, only one of these will ever be at a particular z-position. In other words, if one is at z_0, the other will either not enter the dynamic wavelength until after z_0 (if the new one is older in time) or it will leave the dynamic wavelength before it reaches z_0 (if it is younger in time). All axial points z_0 will be reached by one or the other, unless the particle becomes retrograde or is intercepted by the wall of the drift region. This property is also true if more than two of the same particle are in the dynamic wavelength at the same time. Two particles that are identical (except that one started out one period earlier) can be in a gap region at the same time. The induced current integral includes contributions from both because there is no axial position that both will reach; but between both, all axial distances will be covered. If one were followed strictly (never allowed to leave the wavelength), its extra contributions to the induced current would be identical to that of the other's because the $e^{j\omega t}$ factor in the induced current integral is invariant to changes in the time of an rf period.

It is clear this particle passing must be done self-consistently. The first time particles are transported through the klystron, there is no information about the particles in front that are dropping back and going to be absorbed by the dynamic wavelength we are tracking. However, the ones passing out through the back are known because the position of the trailing edge of the wavelength is well defined. For successive iterations, the particles entering the front are known and a self-consistent solution is possible. Relaxation parameters can be used between successive iterations on the entrance conditions of the particles being overtaken to prevent numerical oscillations. In Fig. 3, a backward-going particle is passed through the dynamic wavelength as a test case.

Simulation Examples

To show the versatility of the code, examples are described that indicate the types of possible physical interpretation for klystron behavior.

In Fig. 4, phase-space diagrams are given that show the effects of detuning the penultimate cavity in a klystron that has a second-harmonic cavity just before the penultimate one. An optimum efficiency, 60%, occurs at a tuning of 816 MHz for 805-MHz operation. The normalized velocity is the instantaneous axial velocity divided by the unmodulated beam velocity. Each vertical set of diagrams is at the drive

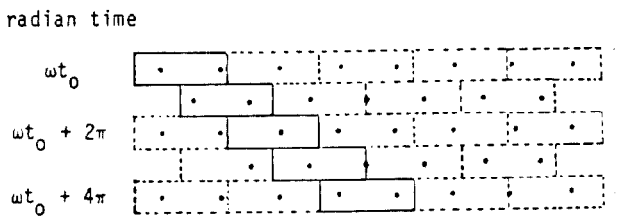

Fig. 3. Represented is a single backward-going particle as it makes its way through the dynamic rf wavelength (the rectangle drawn with the solid lines). Each line shows the wavelength at a different radian time. The rectangles drawn with broken lines show the dynamic rf wavelengths in front of and behind the one followed. As time progresses, the wavelength moves to the right. The different dots on each line show the positions of the retrograde particle, one period apart. Each retrograde particle travels to the lower left corner because they are going backward.

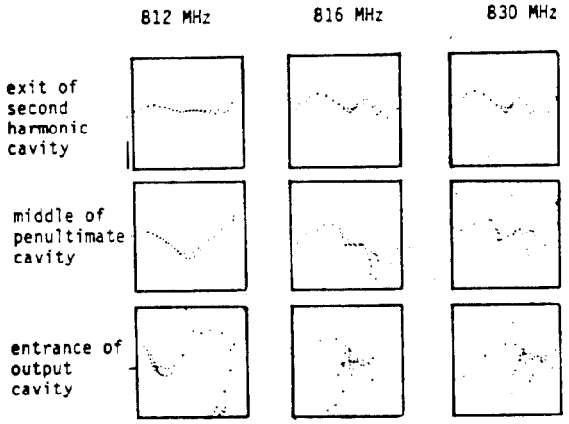

Fig. 4. Velocity-phase diagrams for various detunings of the penultimate cavity. Each set of three diagrams lined up vertically belongs to the same detuning, at different locations in the klystron. The vertical axes refer to axial velocity and the horizontal axes to phase.

level for best efficiency. The effects of too much and too little second-harmonic component in the beam is evident as the penultimate is detuned.

Using the same klystron, effects from the solenoidal magnetic field can be studied. Figure 5 shows the tradeoff between increased efficiency and increased body interception (normalized to overall beam current) as the external axial magnetic field in the output cavity is dropped.

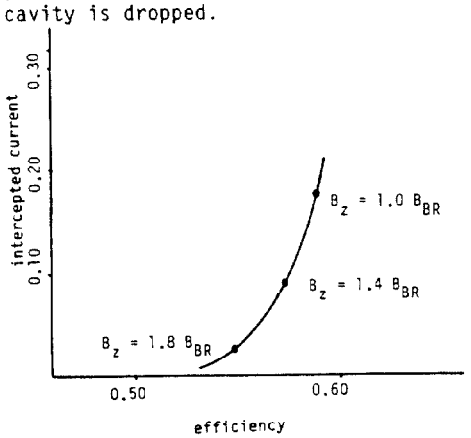

Fig. 5. Intercepted current versus efficiency as the magnetic field in the output cavity is varied. Points corresponding to some of the axial magnetic field values are indicated, with the field in terms of the Brillouin field.

Various initial nonuniform beam-charge densities can be used for the klystron described above. Figure 6 shows normalized charge density versus radial position (where b is the beam's radius) and the best efficiencies for each case (varying the input drive)

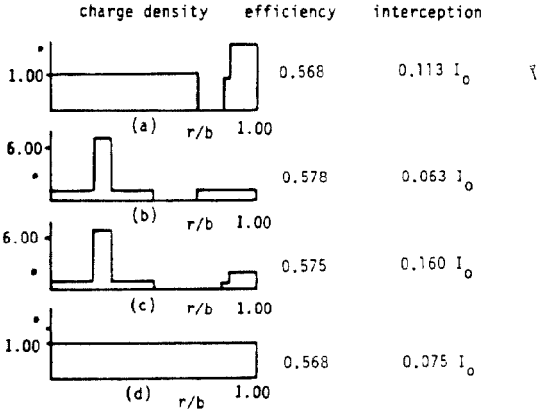

Fig. 6. Nonuniform, charge density of the input beam. Normalized charge density versus normalized radial position and resulting efficiency and body interception. Io is the beam current.

with the corresponding body interception. The body interception depends most critically on the beam scalloping phase when it reaches the output cavity.

Finally, in Fig. 7, power transfer curves are shown for this klystron with a load mismatch VSWR = 4.5 for various phases. The phases refer to the phase on the Smith chart from the smaller resistive side toward the generator. A large amount of experimental data has been taken for this klystron (Litton L-5021, Mod. No. 2007),[4] and excellent agreement is found.

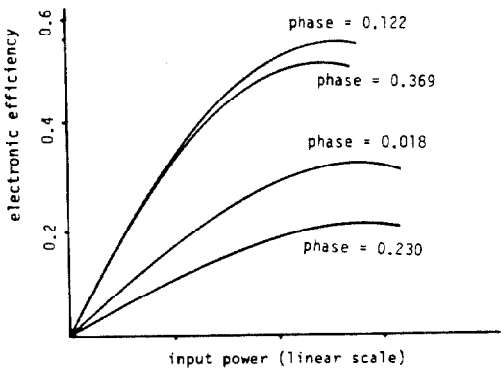

Fig. 7. Computed power-transfer curves for various phases (in the normalized Smith chart units) of a load VSWR = 4.5.

Conclusions

Large-signal klystron simulation has been outlined. Included are a description of iteration schemes to ensure self-consistency and some simulation examples to show the types of klystron analysis possible. The code behaved satisfactorily in all cases, and because of its short running time on a computer, it has been used to design higher efficiency klystrons.

References

1. P. J. Tallerico and B. E. Carlsten, "Computer Modeling of the Klystron," IEEE Trans. on Nucl. Sci. 30 (4) (August 1983), 2170 .

2 K. Halbach, R. F. Holsinger, W. E. Jule, and D. A. Swenson, "Properties of the Cylindrical RF Cavity Evaluation Code SUPERFISH," Proc. 1976 Proton Linear Accelerator Conf., Chalk River Nuclear Laboratories report AECL-5677 (November 1976), 122.

3. B. E. Carlsten, "A Self-Consistent Numerical Analysis of Klystrons using Large-Signal Beam-Wave Interaction Simulations," Ph.D. Thesis, Dept. of Elec. Eng., Stanford University, to be published.

4. R. A. Jameson, R. S. Mills, and R. L. Cody, "Performance of Pulsed 805-MHz, 1.25-MW klystrons into Mismatched Loads," Los Alamos Scientific Laboratory report LA-5649 (September 1974).